

# Multitemporal censusing of a population of eastern hemlock (*Tsuga canadensis* L.) from remotely sensed imagery using an automated segmentation and reconciliation procedure

W. Robert Lamar<sup>a,\*</sup>, James B. McGraw<sup>a</sup>, Timothy A. Warner<sup>b</sup>

<sup>a</sup>Department of Biology, West Virginia University, Morgantown, WV 26506, United States

<sup>b</sup>Geology and Geography Department, West Virginia University, Morgantown, WV 26506, United States

Received 16 January 2004; received in revised form 17 September 2004; accepted 18 September 2004

## Abstract

Large-scale (1:3000) color aerial images of a population of eastern hemlock (*Tsuga canadensis* L.) were collected in the early spring of 1997, 1998, and 1999. An automated spatial segmentation procedure was developed to identify and measure individual population objects or blobs within the forest population. To ensure the comparability of multiyear segmentation maps, an automated blob reconciliation procedure was also developed to make certain that no hemlock pixels were assigned to different blobs in different years. The automated segmentation and reconciliation procedures were applied to a population of naturally occurring hemlock. Following spatial segmentation, a large majority of hemlock blobs (~66–71%) were found to be closely associated with ground referenced, manually delineated individual hemlock crowns. The remaining blobs consisted of spatially distinct parts of a crown or closely clumped multiple crowns. Similar overall classification accuracies (~63–72%) were found following the reconciliation of multitemporal image pairs. The development of these spatially explicit multitemporal population data sets should prove useful to further investigations of the dynamics of and environmental influence on plant populations.

© 2004 Elsevier Inc. All rights reserved.

**Keywords:** Hemlock; Aerial photography; Spatial segmentation; Blob reconciliation; Object-based accuracy assessment

## 1. Introduction

Remote sensing provides ecologists a powerful tool to rapidly obtain spatially explicit data on the vegetation of a large area. At present, high spatial resolution imagery provided by aircraft-based photographic systems appears to provide data at a scale most feasible for study of vegetation change at the population level (Erikson, 2003; Gougeon, 1995; Niemann, 1995; Wulder et al., 2000) although recently launched space-based platforms (i.e., IKONOS and QuickBird) are approaching the resolution required to discern individuals (Kramer, 2002). Given the

potential size of remotely sensed data sets and the extensive time requirements of ground-referenced, manually delineated crown segmentation methods, there exists a basic need to develop an automated segmentation procedure to delineate the individual components of a population.

There have been a number of efforts to develop an automated procedure to segment individual crowns within a tree population. For different forested imagery, the interaction between forest canopy and incident sunlight can result in a variety of different spectral and spatial characteristics to assist in the separation of individual tree crowns. These characteristics vary considerably depending on site, sensor type, image scale, and timing of image collection. Local minima reflectance values, due to shadows between individual crowns (Culvenor, 2002; Gougeon, 1995), local maxima reflectance values representing the tops of upper

\* Corresponding author. Tel.: +1 540 489 4893.

E-mail address: [rlamar@swva.net](mailto:rlamar@swva.net) (W.R. Lamar).

canopy trees (Culvenor, 2002; Pinz, 1991; Pouliot et al., 2002), crown size (Lahav-Ginott et al., 2001), and crown shape characteristics (Pollock, 1998) have all been used to automatically segment individual tree crowns. Most often, a multistep procedure utilizing more than one crown attribute has proven most effective (Brandtberg & Walter, 1998; Culvenor, 2002; Gougeon, 1995; Pinz, 1991; Pollock, 1998; Pouliot et al., 2002).

Phenological differences between hemlock (*Tsuga canadensis* L.) and the neighboring deciduous trees have been used successfully to spectrally segment evergreen and deciduous ground covers (Lamar, 2003). The leaf-off nature of this imagery also allowed us to census a significant portion of the lower canopy segment of the population within the study site. The presence of both sunlit and shaded hemlock crowns, however, resulted in no consistent recognizable radiometric patterns being observed within individual crowns (i.e., local spectral maxima associated with tree apexes).

While there has been some success in the automated segmentation of individual trees from aerial imagery, given the resolution and angular mobility limitations of remote sensing instruments, census data collected from airborne sensors will differ from traditional sampling methods for the foreseeable future. The challenge to ecologists is how to adapt the traditional methods of description and classification to be compatible with the nature of remotely sensed data (Graetz, 1990). The basic unit traditionally used to describe populations has been the individual. Although the genetic identity of this description has many positives, it also presents some difficulties. The clonal nature of many plants blurs the definition of an individual between the whole plant genet and the clonally produced yet potentially independent ramet. Even in nonclonal species, the extensive and complex graft union formed between the roots of different individuals in a number of forest tree species and the subsequent role of these grafts in the translocation of resources suggest a reduced role for individualism with regard to intraspecific competition (Bormann & Graham, 1959). Graham (1959) lists 19 genera and 56 species of forest trees in which natural root grafting has been observed, including eastern hemlock. Still, other trees spread from their base after boles are cut or broken, resulting in multiple crown stems from one genetic individual.

The modular, as opposed to unitary, construction of most plants has long been recognized (Harper, 1976). Using this modular approach, the fundamental unit of a plant population may be regarded as any repeating unit of construction, such as a tree branch or branches (Huenneke & Marks, 1987; McGraw, 1989) or other repeating spatial units (Guardia et al., 2000).

Repeated measurements of the same features over time allow for the investigation of the dynamics of an area's vegetation. "Postclassification comparison" change detection techniques have been used at a pixel level to investigate

the dynamics of wetlands (Jenson et al., 1995), large-scale deforestation (Malingreau & Tucker, 1988), and forest succession (Hall et al., 1991).

Tree and shrub population dynamics can be investigated through repeated measurements of individuals (Enright & Ogden, 1979; Hartshorn, 1975; Martinez-Ramos et al., 1989; Usher, 1972) or parts of individuals (Huenneke & Marks, 1987; McGraw, 1989) within a population over time. "Postclassification comparison" change detection of spatial objects within a population requires a reconciliation of these objects, segmented at different census periods, so that the objects are unique and comparable between census periods.

In this paper, we present a new automated methodology to extract a population data set of hemlock objects from remotely sensed imagery collected in 1997, 1998, and 1999. Our procedure relies on global and local shape and size features to complete spatial segmentation.

Spatial segmentation of hemlock was applied independently to each temporal image. Due to changes in hemlock shapes between years, not all segmentation lines were identical between years. Some hemlock areas were assigned to different objects in different years. Following spatial segmentation, an automated object reconciliation procedure was developed to resolve classification differences and reassign "cross-identified" areas to the same hemlock object for comparable time periods, thus ensuring the meaningful comparison of multitemporal data sets. Reconciliation was performed on paired hemlock image data from 1997–1998 and 1998–1999.

The results from the automated segmentation and reconciliation procedures were compared to a ground-referenced manual crown survey map of the same population.

## 2. Methods

### 2.1. Study area

Our study area is located in the Limberlost-White Oak Canyon area of Shenandoah National Park (38°34' N 78°22' W). This site is located in an upper elevation (951 m) mixed hardwood/hemlock forest. Hemlock is a long-lived, shade tolerant evergreen tree found in many low disturbance eastern United States (US) forests. Established populations usually include a large bank of "saplings", small individuals that may be suppressed beneath a canopy of hemlock or hardwoods for hundreds of years and remain in good condition (Godman & Lancaster, 1990). Like all hemlocks within Shenandoah, the Limberlost-White Oak Canyon population has been adversely impacted in recent years by the presence of the hemlock woolly adelgid (*Adelges tsugae*) whose occurrence was first reported in the park in 1988. This adelgid, believed to inject a toxic saliva into the hemlocks while feeding (Souto et al., 1996), currently infests hemlocks in many eastern US states. Unlike hemlocks in other park locations, most trees within

the study site had only suffered mild to moderate defoliation at the time of aerial sampling. Within the study area, a 3-ha (100×300 m) study plot and an adjoining 0.5-ha (50×100 m) training plot were located. All parameter estimates used in the spatial segmentation and reconciliation procedures were developed using data from the training plot and then applied to the study plot for final analysis.

## 2.2. Image collection, preprocessing, and ground data collection

Large-scale (1:3000) color aerial images of the study area were collected on March 27, 1997, April 13, 1998, and March 31, 1999, using a calibrated Leica/Wild Heerbrugg RC-30 mapping camera with a 300-mm focal length lens. The imagery was acquired before the emergence of new foliage for the deciduous forest component. The color images were scanned at 600 dpi, using an Agfa Dual Scan scanner to produce high resolution (~13 cm/pixel) digital images of the forested study site (Fig. 1). To facilitate comparisons between multitemporal images, image to image geometric registration was performed. Registration using shared primary branch bifurcation points as control points (Herwitz et al., 1998), second-order mapping polynomials and cubic convolution resampling resulted in a root-mean-square (RMS) error of 2.8 pixels (~36 cm) for the 1998/1999 image pair and an RMS error of 2.6 pixels (~34 cm) for the 1997/1998 image pair.

The diameters at breast height (dbh, breast height=1.3 m) of all hemlock trees (dbh ≥5 cm) within the study and training plots were measured in the spring of 1998, using traditional field methods.

## 2.3. Manual crown segmentation

Manual delineation of irregularly shaped tree crowns on large-scale imagery is usually not free of error. Measurements of isolated tree crowns using spectral segmentation procedures have been found to produce more accurate estimates of size than manual delineation (Lahav-Ginott et

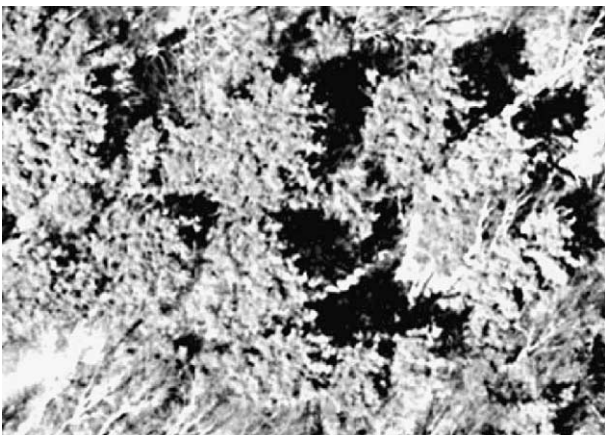


Fig. 1. Section of study site from March 1997 image.

al., 2001). For this reason, initial map preparation involved spectrally separating the evergreen vegetation of the study site from other ground covers. Spectral segmentation used a maximum likelihood classification algorithm and a global fused class decision-making process that applied the summarized decisions of local class statistics derived from all 3 years of radiometrically normalized imagery to each year's image (Lamar, 2003).

The boundaries between individual hemlock crowns and the boundaries between hemlock crowns and other types of evergreen vegetation were manually delineated in the field from these spectrally segmented vegetation maps. Manual delineation was aided by the use of multiple years of aerial imagery and multiple images from different viewing angles each year. The manual crown survey map was produced in the spring of 1998 from the 1998 images. All comparisons of the automated aerial censuses in this study were thus made with respect to this 1998 manual crown survey map. A full description of the hemlock population within the study area based both on ground-collected and ground-referenced aerial-collected data has been previously described (Lamar, 2003).

## 2.4. Automated spatial segmentation

Our automated spatial segmentation procedure was applied independently to each of the multitemporal spectrally segmented vegetation maps of the study site. The objective of this procedure was to divide the hemlock component of the aerial imagery into distinct population features based on shape and size. Spatial segmentation was a five-step process including shadow thresholding, Euclidean distance map (EDM) construction and smoothing, watershed segmentation, and small blob joining.

### 2.4.1. Shadow thresholding

Shadows can both assist and hinder crown segmentation efforts (Brandtberg & Walter, 1998; Gougeon, 1995; Pollock, 1998). On one hand, the intercrown shadows, by providing a distinct edge around the perimeter of an individual tree crown, can greatly assist efforts to delineate that crown from its adjacent neighbors. Conversely, shadows can hide valuable information about the true nature of a crown's shape and size. A single tree, when intercepted by intracrown shadows, can be mistaken for several separate trees by both automated and manual segmentation procedures.

To investigate the nature of the shading within the study area, all inter and intracrown shadows within the training plot were manually identified and mapped during the preparation of the manual crown survey map. The size differences between inter and intracrown shadows were examined using a Wilcoxon rank sum test (Wilcoxon, 1945). To distinguish inter and intracrown shadows for automated segmentation, an optimal threshold shadow size was determined through a systematic trial of a range of

shadow sizes. The size that produced the maximum overall accuracy following watershed segmentation (Soille, 2003) was defined as the optimal threshold size. All shadows below this threshold were filled in as hemlock before automated watershed segmentation of the study plot. These shadows were then added back to the image prior to further segmentation, reconciliation, and analysis.

For multitemporal comparisons, the presence of shadows presents another challenge. At the pixel level, the transition between hemlock and other nonshadow ground covers from one sampling time to another is considered an actual change. The transition between hemlock and shadow, however, represents an unknown. The shadow could be masking a hemlock pixel, in which case no actual change has occurred, or the shadow could be masking an actual change between hemlock and another ground cover. Due to the level of uncertainty for these transitions, all pixels within each image pair exhibiting this transition were eliminated as hemlock prior to spatial segmentation. This had the effect of adding 1997 and 1998 shadows to both images within the 1997–1998 image pair. Likewise, 1998 and 1999 shadows were added to both images of the 1998–1999 image pair.

Studies have shown a significant statistical relationship between ground and aerial measurements of tree size from single time period images (Aldred & Sayn-Wittgenstein, 1972; Hagan & Smith, 1986; Minor, 1951). The addition of another year of shadows to each image within an image pair, however, could potentially increase the masking of the aerial crown measurements. The relationship between ground measurements of size (dbh) and aerial measures of size (crown area) for the 1998 hemlock crowns within the 1997–1998 and 1998–1999 image pairs was investigated using correlation analysis.

2.4.2. EDM construction and Gaussian smoothing

EDMs were constructed by performing a distance transform on the spectrally classified binary image, assigning a

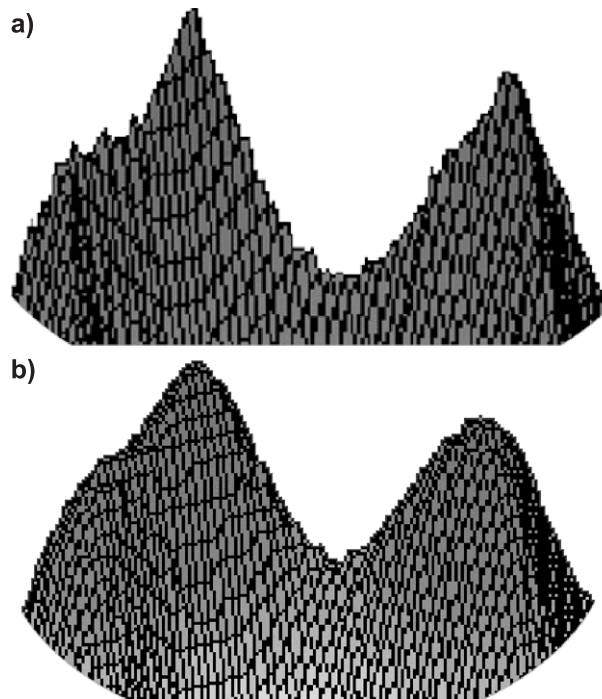


Fig. 3. Effects of EDM smoothing. (a) Original EDM and (b) smoothed EDM.

brightness value to each hemlock pixel corresponding to the pixel’s Euclidean distance from its nearest boundary (see Russ (1995) for further description of this procedure). Local maxima on the EDM represent the center or peak of a hemlock clump; local minima represent edge pixels (Fig. 2). Effective spatial division of an EDM using the watershed segmentation method depends on the orderly relation of gray scale pixel values. Typically, this pixel relationship is the result of an EDM constructed from convex or mostly convex shapes. Less convex shapes and local boundary irregularities lead to a surplus of local maxima and oversegmentation.

To minimize oversegmentation, a Gaussian filter with a standard deviation ( $\sigma$ ) of 0.65 pixels was applied to the

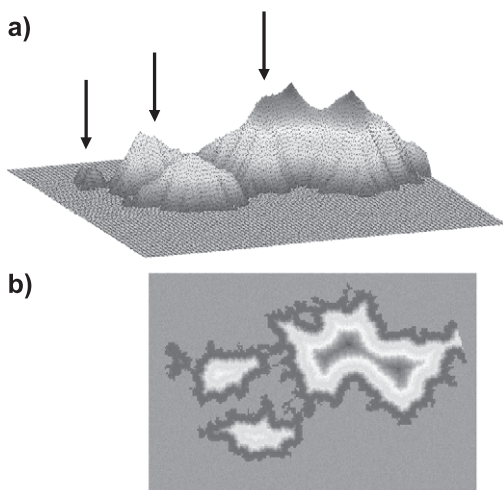


Fig. 2. Hemlock clump following Euclidean distance mapping, (a) 3-D view with arrows pointing to false maxima and (b) 2-D view.

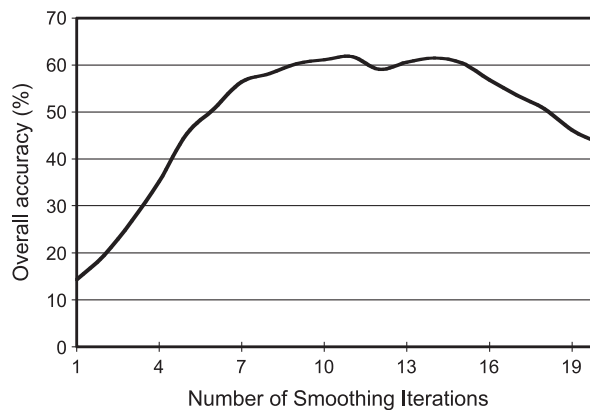


Fig. 4. Effect of varying the number of Gaussian smoothing iterations on overall accuracy, training plot, 1998 data from 1998–1997 and 1998–1999 image pairs.

EDM prior to watershed segmentation to remove excess local maxima (Fig. 3). To minimize the possible effects of neighbors on the smoothing of a feature, the Gaussian filter was truncated as a  $5 \times 5$  kernel. The degree of smoothing needed to achieve the highest overall accuracy was investigated through a systematic trial of smoothing iterations within the training site (Fig. 4). The number of smoothing iterations, which resulted in highest overall hemlock classification accuracy in the training site, was then applied to the study site data for final analysis.

#### 2.4.3. Watershed segmentation

Beucher and Lantuejoul (1979) introduced the idea that by viewing the intensity of any gray-scale image as elevation and simulating runoff, it is possible to decompose an image into watershed regions. In our study, watershed analysis was performed using the public domain NIH ImageJ program (U.S. National Institute of Health, 2003) and based on the algorithm described by Soille (2003). Intuitively, the concept of watershed can be explained in terms of flooding. The EDM is inverted so that local maxima are now local minima. Starting at the minima, water progressively floods the catchment basins of the image. At the places where the waters coming from two different minimums would merge, a dam is raised. Following the flooding procedure, each minimum and associated catchment basin is segmented by dams from adjacent catchment basins. Hereafter, we shall refer to these basins consisting of one local minimum and a support region of significantly darker pixels than its neighborhood as blobs (Lindeberg, 1994).

#### 2.4.4. Small blob joining

Even with EDM smoothing, the watershed method produced excessive hemlock segmentation due to the presence of large irregular crown branches and intracrown shadows. To improve the overall classification accuracy, a small blob joining procedure was applied following watershed segmentation. This procedure identified an optimal small blob size and joined each blob below this size with its contiguous neighbor with whom it shared the largest common boundary. The optimal small blob joining size was determined from the training data through a systematic trial of different blob sizes to identify the joining size where overall accuracy was maximized.

#### 2.5. Automated blob reconciliation

The automated spatial segmentation procedure was used to segment blobs within the 1997–1998 and 1998–1999 image pairs. Because of variations in viewing geometry, as well as real changes in the hemlock canopy, not all segmentation lines were identical in the different images of an image pair. Some hemlock areas were assigned to different blobs in different years. This condition makes no biological sense in as much as hemlock branches cannot

switch trees, and it complicates the tracking of unique blobs over time. An automated procedure, which we term blob reconciliation, was developed to identify areas assigned to different blobs in different years of an image pair, resolve these classification differences, and reassign “cross-identified” areas to the same blob for comparable time periods, thus ensuring the meaningful comparison of multitemporal data sets.

##### 2.5.1. Patch identification

As an initial step of reconciliation, the image pair to be reconciled (images at time  $t$  and  $t+1$ ) were overlaid, and areas of connected hemlock pixels were classified according to their classification on both images as (1) joint-year areas, identified as hemlock at both  $t$  and  $t+1$  or (2) single-year areas, identified as hemlock at either but not both time  $t$  and  $t+1$  (Fig. 5a and b). Joint-year areas assigned to different

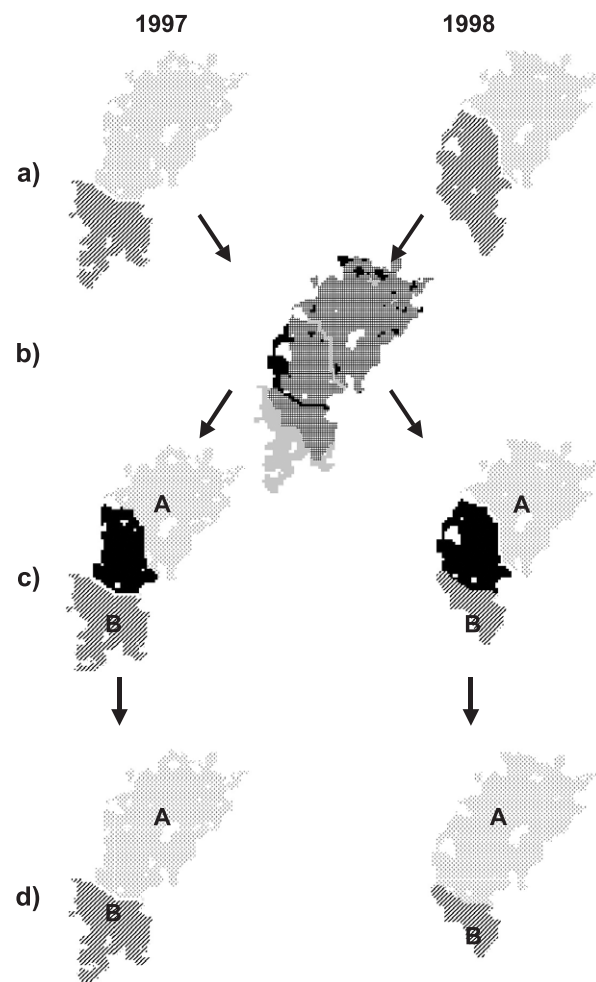


Fig. 5. Reconciliation process. (a) Segmented (but not reconciled) blobs from 1997 and 1998 image pair, (b) overlaid images with pixels classified as joint-year (grid lines), single-year (1997) only (gray), or single-year (1998) only (black). (c) Areas not needing reconciliation are passed to reconciliation base maps as Blobs A and B. Areas to be considered for reconciliation grouped as patch (black) on both 1997 and 1998 image (d) reconciled patch assigned to Blob A (with which the greatest connectivity was shared).

blobs at time  $t$  and  $t+1$  were differentiated from joint-year areas that were assigned to the same blobs at both times. No crown reconciliation was necessary for these later areas and also for any connected single-year area with which they shared a greatest common boundary. Likewise, no reconciliation was needed for single-year areas not connected to any joint-year areas. These areas, where reconciliation was not needed, were added unaltered to reconciliation base maps  $t$  and  $t+1$  (Fig. 5c). These nonreconciled areas represented the large majority of all pixels within all image pairs (68.6–72.2%). Areas to be considered for reconciliation were grouped into spatially connected regions termed patches. Each patch was comprised of one cross-identified joint-year area (identified, for example, with Blob A at time  $t$  and with Blob B at time  $t+1$ ) and any single-year areas with which it shared a greatest common connected boundary. For example, a patch from the 1997 image consisted of a joint-year area and all single-year (1997 only) areas with which it shared a greatest common connected boundary. The corresponding patch from the 1998 image consisted of the same joint-year area and all single year (1998 only) areas with which it shared a greatest common connected boundary.

### 2.5.2. Patch–blob connectivity

Reconciliation decisions about these patches were based on the relative strength of the connection or connectivity between patch and the patch's neighboring blobs on both images of an image-pair. For a patch assigned to Blob A at time  $t$  and Blob B at time  $t+1$ , this meant assessing the patch connectivity to both neighboring blobs at both times of an image pair.

The connectivity between patch ( $i$ ) and neighboring blob ( $A$ ) was measured on both images of an image pair as the weighted ratio of common boundary region and patch size such that:

$$\text{Connectivity}(i, A) = \frac{(\text{CBR}_{i,A,(t)} + \text{CBR}_{i,A,(t+1)})}{\left(P_{i,(t)} + P_{i,(t+1)}\right)^2} \quad (1)$$

where  $\text{CBR}_{i,A,(t)}$  is the common boundary region of patch ( $i$ ) and neighboring blob ( $A$ ) on time  $t$  image,  $\text{CBR}_{i,A,(t+1)}$  is the common boundary region of patch ( $i$ ) and neighboring blob ( $A$ ) on time  $t+1$  image,  $P_{i,(t)}$  is the size of patch ( $i$ ) on time  $t$  image, and  $P_{i,(t+1)}$  is the size of patch ( $i$ ) on time  $t+1$  image.

The CBR between a considered patch and its neighboring blob was identified from a scanning operation as the sum of all patch pixels found within a moving  $7 \times 7$  window centered on the edge pixels of the neighboring blob. Viewing geometry differences between images can result in “pseudochanges” in the hemlock canopy that cause the relative positions of patches and neighboring blobs to appear to be slightly off-set between years. Real changes in hemlock canopy shape between images can also change

the relationship between patch and neighboring blobs. These real or pseudochanges could create a situation where a patch may be strongly associated with a neighboring blob on one image but appear to be slightly separated from the same neighboring blob on the second of an image pair. The  $7 \times 7$  window size used in the boundary scan permitted a patch within close proximity but not connected to a neighboring blob at one image time to be considered for possible inclusion with that blob during reconciliation.

The neighboring blob sharing the maximum connectivity with a patch was termed the patch's greatest common neighboring blob.

### 2.5.3. Reconciliation decision making

Following calculations of each patch's connectivity, the patch was subjected to a decision-making procedure (Fig. 6). From a systematic trial of the training data, a threshold connectivity value ( $\Psi$ ) was obtained that maximized the overall classification accuracy of the training site hemlock. If the patch's greatest connectivity  $< \Psi$ , then the patch was deemed to lack a significant connection with any neighboring blobs and was assigned as a new and unique blob on base maps  $t$  and  $t+1$ . If the patch's greatest connectivity  $\geq \Psi$ , then the patch was added on base map  $t$  and  $t+1$  as a part of its greatest common neighboring blob (Figs. 5d and 7).

The automated blob reconciliation procedure was used to reconcile segmented hemlock blobs in each image of the 1997–1998 and 1998–1999 image pairs.

### 2.6. Blob threshold size

The manual crown survey found that many of the smallest evergreen blobs within the aerial imagery were separated at such a distance from all identified hemlock crowns that they could not be linked with certainty to any one crown. These smallest blobs represented isolated hemlock branches cut off from the main crown by shadows or other ground covers, crowns belonging to hemlocks with a dbh of  $< 5$  cm, or branches of mountain laurel (*Kalmia latifolia*) whose canopies, because of internal shading, tended to be dissected into small discontinuous patches. Because of the uncertain identity and relative insignificance

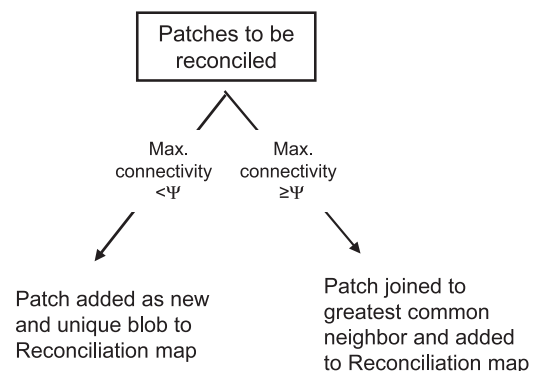


Fig. 6. Reconciliation decision making.

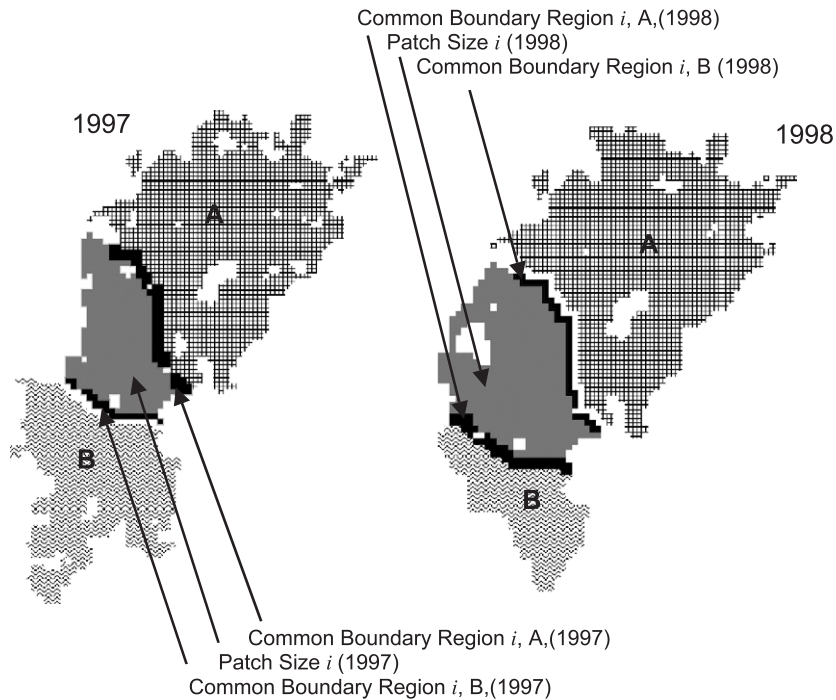


Fig. 7. Reconciliation procedure considers patch  $i$  (gray) that has been segmented into different blobs for 1997 and 1998. The difference in blob assignment between image years was due to the change in size and shape of blob B in 1998 due to an ice storm. Connectivity between patch and blobs was calculated (using Eq. (1)). Blob A was found to be the patch's greatest common neighbor. In as much as the patch's greatest connectivity (with Blob A)  $\geq \Psi$ , the patch was assigned to Blob A on both 1997 and 1998 maps (see Fig. 5d).

of these smallest blobs, a blob threshold size was developed. Only blobs above this threshold were considered for further comparison and description. The blob threshold was selected based on the smallest crown size predicted from the minimum ground-based dbh measurement and the least squares regression of crown size and dbh.

### 2.7. Accuracy assessment—automated segmentation and reconciliation

Unlike pixel-based accuracy assessments that have achieved at least some level of standardization over time (Congalton, 1991), the accuracy assessments of object-based segmentation efforts have generally been quite limited and varied. The type of assessment performed is often dependent on the objectives of the study and the type of ground-referenced data available for comparison. One type of assessment, which we term whole plot accuracy, compares the total number of manually delineated crowns or counted stems with the total number of automatically delineated blobs within a designated area. Whole plot assessments are often used when the only available description of the study area may be a measure or estimate of tree density. While useful for some stand level descriptions and monitoring activities, whole plot assessments generally provide a poor measure of “true” accuracy due to the canceling actions of individual tree errors of omission and commission.

Methodologies assessing the 1:1 correspondence of “individuals” (in our case, automated blobs and manually delineated crowns) provide a much more useful measure of accuracy (Leckie & Gougeon, 1998), particularly for demographic studies. Unlike pixel-based or count-based accuracy assessments, object-based assessments face added difficulties, having to make comparisons between features that lack uniform size and positional equivalency on comparison images. Given these differences, one must initially define when a crown and a blob have achieved 1:1 correspondence. In this study, we defined 1:1 correspondence as occurring when the overlap area between a manually delineated crown and an automated blob includes  $\geq 50\%$  of both features' total size.

Using this definition, several descriptive measures of the blob–crown relationship can be obtained (Fig. 8). Two common assessments of pixel-based classifications are user's and producer's accuracy. These assessments can be adapted to object-based classifications. User's accuracy, indicative of the probability that an automated blob achieves 1:1 correspondence with a manually delineated crown, can be defined such that:

User's accuracy

$$= \frac{\# \text{ of } 1 : 1 \text{ blob:crown correspondences}}{\text{Total } \# \text{ blobs obtained from automated segmentation}} \quad (2)$$

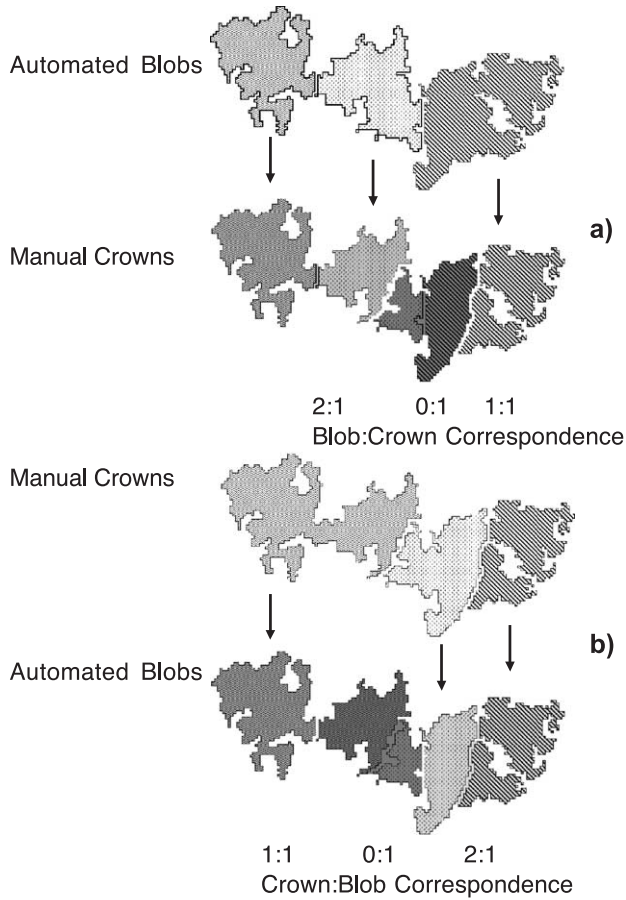


Fig. 8. Accuracy assessment using 1:1 correspondence. (a) Overlays automated blobs on manual crowns. Arrows point to crowns, which contain  $\geq 50\%$  of overlaid blob. Producer's accuracy=(1) 1:1 crown/blob correspondences/3 total crowns=33%. (b) Overlays manual crowns on automated blobs. Arrows point to blobs, which contain  $\geq 50\%$  of overlaid crown. User's accuracy=(1) 1:1 blob/crown correspondences/3 total blobs=33%. Overall accuracy=(2) 1:1 blob:crown and 1:1 crown:blob correspondences and crowns=33%. Interestingly and, perhaps misleadingly, whole plot accuracy for this example is 100% (3 crowns/3 blobs).

Producer's accuracy, which is a measure of the probability that a manually delineated crown achieves 1:1 correspondence with an automated blob, is defined as:

$$\text{Producer's accuracy} = \frac{\# \text{ 1 : 1 crown:blob correspondences}}{\text{Total \# crowns obtained from manual segmentation}} \quad (3)$$

An assessment of the crown–blob relationship using either user's or producer's accuracy alone can be misleading as errors of overaggregation and overdissection result in different blob–crown and crown–blob correspondences. For example, three manually delineated crowns aggregated into one blob results in one 3:1 crown–blob correspondence from the user's perspective but three 0:1 crown–blob correspondences from the producer's perspective. Is it more helpful to consider this situation as one crown overaggregation error or

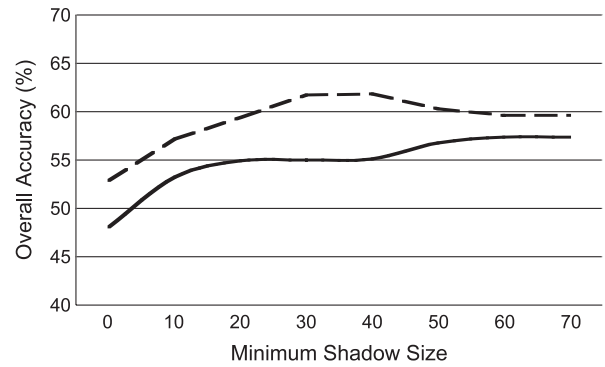


Fig. 9. Effect of varying threshold shadow size on overall accuracy, training plot, 1998 data from 1998–1997 image pair and 1998–1999 image pair.

three blob overdissection errors? Congalton (1991) suggests that a measure of overall accuracy has advantages over either user's or producer's accuracy. Overall accuracy permits one to more fully understand the relationship between manually delineated crowns and automated blobs by describing the relationship from both perspectives. This accuracy assessment, the probability that both a manually delineated crown and automated blob have 1:1 correspondence with each other, is defined as:

$$\text{Overall accuracy} = \frac{\# \text{ of 1 : 1 blob:crown} + \# \text{ of 1 : 1 crown:blob correspondences}}{\text{Total blobs} + \text{Total crowns}} \quad (4)$$

In this study, segmentation and reconciliation parameters (threshold shadow size, blob joining size, and threshold connectivity) were determined from empirical trials by selecting values that maximized overall accuracy in the training data. Overall accuracy is also calculated to describe the effectiveness of the segmentation and reconciliation procedures on the 1997–1998 and 1998–1999 image pairs in comparison to the 1998 manual crown survey map.

### 3. Results

A good correlation ( $r=0.759$ ) was found between measurements of 1998 hemlock size in the air (crown area)

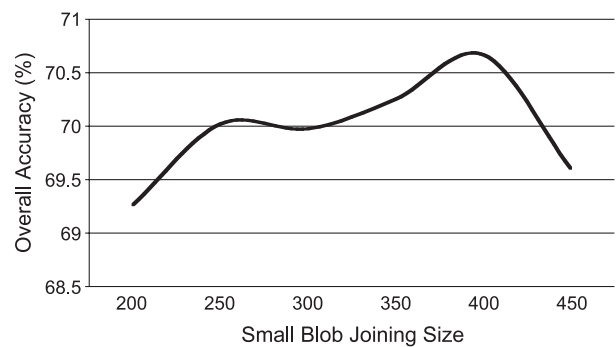


Fig. 10. Effect of varying small blob joining size on overall accuracy, training plot, 1998 data from 1998–1997 and 1998–1999 image pairs.



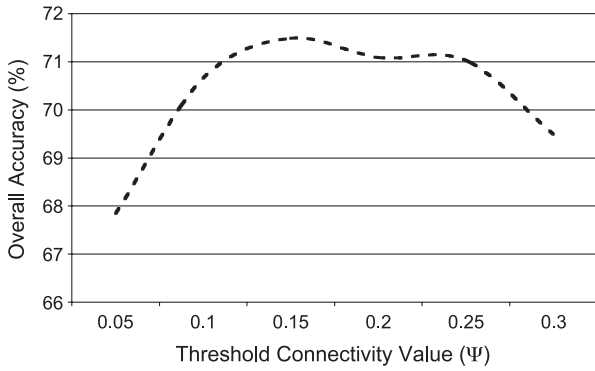


Fig. 11. Effect of varying threshold connectivity values on overall accuracy, training plot, 1998 data from 1998–1997 and 1998–1999 image pairs.

on both 1997–1998 and 1998–1999 image pairs and on the ground (dbh) despite the elimination of all pixels exhibiting hemlock–shadow transitions within each image pair map. This correlation was similar to the correlation ( $r=0.776$ ) found between the same two size measures on the 1998 imagery without shadows added (Lamar, 2003).

The regression of crown area on dbh produced a regression equation of:

$$\text{Crown Area (in pixels)} = 37.6585 + 28.0415 \text{ dbh} \quad (7)$$

Substituting the minimum ground sampling size (dbh) of 5 cm into the regression equation resulted in a blob threshold size of 178 pixels (diameter ~2 m). Contiguous hemlock patches below this size, many of which could not be accurately traced to any single hemlock crown, were considered noise and eliminated from further consideration.

The size of intra and intersize shadows, as identified in the training plot, differed significantly. Intracrown shadows were found to be significantly smaller than intercrown shadows for 1998 hemlocks on both the 1997–1998 and 1998–1999 image pairs (Wilcoxon rank sum test,  $p < 0.0001$  for both pairs). The results of a systematic trial of threshold shadow sizes showed overall classification accuracy to initially improve as the threshold shadow size was increased (Fig. 9). As small intracrown shadows were filled, the number of automated blob overdissection errors (a blob comprised of part [ $<50\%$ ] of a crown) decreased. As threshold shadow size continued to increase, however, overall accuracy began to decrease with the closure of intercrown shadows. The closure of these shadows caused an increase in the number of blob overaggregation errors (a blob comprised of multiple crowns.) Optimal threshold shadow

Table 1  
Accuracy assessment—automated blob segmentation procedure (1998 data for 1997–1998 image pair) compared to 1998 manual crown survey map

	Correspondence				
	4:1	3:1	2:1	1:1	0:1
Aerial accuracy (crowns–blob)	0	15	61	340	59
Ground accuracy (blobs–crown)	0	1	41	366	117

Overall accuracy=706/1000=70.6%.

Table 2  
Accuracy assessment—automated blob segmentation procedure (1998 data for 1998–1999 image pair) compared to 1998 manual crown survey map

	Correspondence				
	4:1	3:1	2:1	1:1	0:1
Aerial accuracy (crowns–blob)	2	11	62	339	90
Ground accuracy (blobs–crown)	0	3	55	351	126

Overall accuracy=690/1039=66.4%.

size was the size that minimized both types of segmentation problems resulting in the highest overall classification accuracy for hemlocks within the training plot. This optimal size was found to be 40 pixels (diameter=90 cm) for 1997–1998 data and 55 pixels (diameter ~1 m) for 1998–1999 data.

The pattern of balancing errors of blob (and crown) overaggregation and overdissection was also found in systematic trials of different small blob joining sizes (Fig. 10) and threshold connectivity values (Fig. 11) within the training plot. As blob joining size and threshold connectivity increased, blob overdissection decreased. As blob joining size and threshold connectivity continued to increase, however, errors of blob overaggregation began to increase. A balancing of these errors resulted in highest overall classification accuracy. For small blob joining, this size was found to be 400 pixels (diameter=2.87 m). All smaller hemlock blobs were joined to their contiguous neighbor, if present, with whom they shared the largest common boundary. For threshold connectivity, a value of 0.00015 produced the highest overall accuracy. Patches with maximum connectivity values smaller than this threshold were added to the reconciliation base map as new and unique blobs.

The accuracy of the automated segmentation procedure was compared to the 1998 manual crown survey map. Two automated maps from 1998, one associated with the 1997–1998 image pair and another with the 1998–1999 image pair, were compared to the survey map. The difference between these two 1998 maps was the inclusion of 1997 shadows with the 1997–1998 image pair and 1999 shadows with the 1998–1999 image pair. Findings show that 1998 automated blobs and 1998 manually delineated crowns had 70.6% 1:1 correspondence in the 1998–1997 image pair and 66.4% 1:1 correspondence in the 1998–1999 image pair (Tables 1 and 2).

Assessing the accuracy of the automated reconciliation procedure in comparison to the 1998 manual crown survey map showed 1998 manually delineated crowns and 1998

Table 3  
Accuracy assessment—automated blob reconciliation procedure (1998 data for 1997–1998 image pair) compared to 1998 manual crown survey map

	Correspondence				
	4:1	3:1	2:1	1:1	0:1
Aerial accuracy (crowns–blob)	0	8	64	355	69
Ground accuracy (blobs–crown)	0	15	61	340	59

Overall accuracy=695/971=71.6%.

Table 4

Accuracy assessment—automated blob reconciliation procedure (1998 data for 1998–1999 image pair) compared to 1998 manual crown survey map

	Correspondence				
	4:1	3:1	2:1	1:1	0:1
Aerial accuracy (crown–blob)	2	8	52	357	147
Ground accuracy (blob–crown)	2	14	73	339	107

Overall accuracy=696/1101=63.2%.

reconciled blobs had 71.6% 1:1 correspondence for the 1998–1997 image pair and 63.2% 1:1 correspondence for the 1998–1999 image pair (Tables 3 and 4).

#### 4. Discussion

The segmentation of a remotely sensed tree population into individual crowns presents a considerable challenge. While the results of this study are compatible with other studies completed in mature natural forest stands (Leckie & Gougeon, 1998), approximately 1/3 of the hemlock blobs segmented in the automated procedures and hemlock crowns from the manual crown survey map did not achieve 1:1 correspondence. Numerous problems confront the spatial segmentation of individual crowns. Forked branches or crowns dissected by hardwood branches and shadows cause a spatial separation between crown segments that often leads to the overdissection of an individual crown into multiple blobs. Conversely, the lack of spatial separation between neighboring tree crowns can lead to the overaggregation of several individual crowns into one blob. The architecture of hemlock branching, particularly the branching of individuals in the lower canopy, accentuated these segmentation problems, with the wide spreading and quite flexible hemlock branches often becoming intertwined with neighboring crowns. For our multiple canopy level imagery, adjacent neighbors, if occupying different levels of the canopy, do not have to be in direct physical contact with each other to appear to be overlapping in the aerial images. Interestingly, despite the segmentation difficulties illustrated by our 1:1 correspondence assessment, whole plot accuracy levels were quite high for the segmentation procedure (90.5–94.2%) and reconciliation procedure (94.5–95.8%) applied to both 1997–1998 and 1998–1999 image pairs. These high accuracy figures seem to highlight both the value of the automated procedures for some types of monitoring situations and the need to clearly describe how the accuracy of any segmentation procedure was assessed.

Previous postclassification change detection studies have encountered problems due to the compounding of classification errors for the multitemporal imagery (Pilon et al., 1988). While pixel-based errors in this study may be subject to similar error compounding, its impact is lessened by the high overall accuracy (>92%) of spectral classification (Lamar, 2003). The accuracy of multitemporal object-based classification can also be negatively affected by the

compounding of segmentation errors from both multitemporal images into each multitemporal image. The challenge for reconciliation is to determine which contradictory segmentation lines within multitemporal image pairs should be included to maximize overall classification accuracy. We adopted a best fit approach towards this challenge by measuring the connectivity of reconcilable patches from the perspective of both multitemporal images. Reconciliation accuracy also benefits by considering a patch's spectral classification history (joint or single-year pixels). The result is that overall classification accuracy for both image pairs following reconciliation is only slightly different than accuracy prior to reconciliation (+1.0% and -3.2% for 1998 maps from 1997–1998 and 1998–1999 image pairs).

In this study, we presented both an automated methodology for extracting a population data set from remotely sensing imagery and a description of the relationship between blobs viewed from the air and individual tree crowns. Each hemlock blob consists of a distinct portion of hemlock crown canopy segmented from its neighbors on the basis of size, shape, and connectivity. Besides their described quantitative relationship, blobs classified from aerial imagery and individual trees censused on the ground share many other similarities. Like an individual, the fate of a blob can be followed over time; both blobs and individuals can be born, grow, regress, or die over time. In the case of blobs, "birth" is not the product of recent germination as is the case with individuals. Rather, a "birth" into aerial view is typically the emergence of a previously suppressed individual(s) into the canopy as the result of a canopy disturbance. Importantly, from an ecological perspective, both blobs and individuals can influence their surrounding environments and compete for resources with their neighbors. The development of a multitemporal data set allows for the following of unique blobs over time. From such a data set, the parameters needed for demographic population modeling can be extracted and a population's dynamics and influences over time investigated. The spatially explicit nature of this data set permits the incorporation of environmental variables, such as topography, soils, and climate into the demographic modeling.

Spatial resolution advances in space-based, remote sensing devices will result in future subcontinental and continental scale data sets that can be "mined" for demographic information on trees, shrubs, and other plants of interest. Therefore, explicit considerations of the relationship between "individuals" (i.e., blobs) as seen from above and true individuals in the global population of a species will become important. The future availability of huge, spatially explicit, remotely sensed, population data sets should assist investigations within a number of diverse areas of study, such as rare plant conservation, intraspecific plant interactions, and the effects of spatial and temporal environmental variability including global climate change effects on plant dynamics.

## References

- Aldred, A. H., & Sayn-Wittgenstein, L. (1972). Tree diameters and volumes from large scale aerial photographs. *Photogrammetric Engineering*, 38, 871–873.
- Beucher, S., & Lantuejoul, C. (1979). Use of watersheds in contour detection. *International workshop on image processing, conference* (pp. 12–21). Rennes, France: CCETT/INSA/IRISA.
- Bormann, F. H., & Graham, B. F. (1959). The occurrence of natural root grafting in eastern white pine. *Pinus strobus* and its ecological implications. *Ecology*, 40(4), 677–691.
- Brandtberg, T., & Walter, F. (1998). An algorithm for delineation of individual tree crowns in high spatial resolution aerial images using curved edge segments at multiple scales. *International forum: Automated interpretation of high spatial resolution digital imagery for forestry, Conference Natural Resources Canada, Victoria, British Columbia* (pp. 41–54).
- Congalton, R. G. (1991). A review of assessing the accuracy of classifications of remotely sensed data. *Remote Sensing of Environment*, 37, 35–46.
- Culvenor, D. S. (2002). TIDA: An algorithm for the delineation of tree crowns in high spatial resolution remotely sensed imagery. *Computers & Geosciences*, 28, 33–44.
- Enright, N., & Ogden, J. (1979). Applications of transition matrix models in forest dynamics; *Araucaria* in Papua New Guinea and *Nothofagus* in New Zealand. *Australian Journal of Ecology*, 4, 3–23.
- Erikson, M. (2003). Segmentation of individual tree crowns in colour aerial photographs using region growing supported by fuzzy rules. *Canadian Journal of Forest Resources*, 33, 1557–1563.
- Godman, R. M., & Lancaster, K. (1990). *Tsuga canadensis*. In B. H. Honkala (Ed.), *Silvics of North America, Vol. 1. conifers* (pp. 41–51). Washington, DC: US Department of Agriculture.
- Gougeon, F. A. (1995). A crown-following approach to the automatic delineation of individual tree crowns in high spatial resolution aerial images. *Canadian Journal of Remote Sensing*, 21(3), 274–284.
- Graetz, R. D. (1990). Remote sensing of terrestrial ecosystem structure: An ecologist's pragmatic view. In R. J. Hobbs, & H. A. Mooney (Eds.), *Remote sensing of biosphere functioning* (pp. 41–51). New York: Springer-Verlag.
- Graham, B. F. (1959). *Root-grafts in eastern white pine, Pinus strobus L.; Their occurrence and ecological implications*. PhD Durham, NC, Duke University.
- Guardia, R., Raventos, J., & Caswell, H. (2000). Spatial growth and population dynamics of a perennial tussock grass (*Achnatherum calamagrostis*) in a badland area. *Journal of Ecology*, 88, 950–963.
- Hagan, G. F., & Smith, J. L. (1986). Predicting tree groundline diameter from crown measurements made on 35-mm aerial photography. *Photogrammetric Engineering and Remote Sensing*, 52(5), 687–690.
- Hall, F. G., Botkin, D. B., Strelbel, D. E., Woods, K. D., & Goetz, S. J. (1991). Large-scale patterns of forest succession as determined by remote sensing. *Ecology*, 72(2), 628–640.
- Harper, J. L. (1976). The concept of population in modular organisms. In R. M. May (Ed.), *Theoretical ecology. Principles and applications* (pp. 53–77). Oxford: Blackwell Scientific Publications.
- Hartshorn, G. S. (1975). A matrix model of tree population dynamics. In F. B. Golley, & E. Medina (Eds.), *Tropical ecological systems* (pp. 41–51). New York: Springer-Verlag.
- Herwitz, S. R., Slye, R. E., & Turton, S. M. (1998). Co-registered aerial stereopairs from low-flying aircraft for the analysis of long-term tropical rainforest canopy dynamics. *Photogrammetric Engineering and Remote Sensing*, 69(5), 397–406.
- Huenneke, L. F., & Marks, P. L. (1987). Stem-dynamics of the shrub *Alnus incanta* ssp. *rugosa*: Transition matrix models. *Ecology*, 68, 1234–1242.
- Jenson, J. R., Rutchey, K., Kock, M. S., & Narumalani, S. (1995). Inland wetland change detection in the Everglades Water Conservation Area 2A using a time series of normalized remotely sensed data. *Photogrammetric Engineering and Remote Sensing*, 61(2), 199–209.
- Kramer, H. J. (2002). *Observation of the earth and its environment—survey of missions and sensors*. Springer-Verlag. 1510 pp.
- Lahav-Ginott, S., Kadmon, R., & Gersani, M. (2001). Evaluating the viability of *Acacia* populations in the Negev Desert: A remote sensing approach. *Biological Conservation*, 98(2), 127–137.
- Lamar, W. R. (2003). *Censusing and modeling a population of eastern hemlock (Tsuga canadensis L.) using remote sensing*. Ph. D thesis Biology Department, Morgantown, WV, West Virginia University.
- Leckie, D. G., & Gougeon, F. A. (1998). An assessment of both visual and automated tree counting and species identification with high spatial resolution multispectral imagery. *International forum: Automated interpretation of high spatial resolution digital imagery for forestry Victoria, British Columbia* (pp. 141–152).
- Lindeberg, T. (1994). *Scale-space theory in computer vision*. Boston: Kluwer Academic Publishers.
- Malingreau, J. P., & Tucker, C. J. (1988). Large-scale deforestation in the southeastern Amazon Basin of Brazil. *Ambio*, 17, 49–55.
- Martinez-Ramos, M., Alvarez-Buylla, E., & Sarukhan, J. (1989). Tree demography and gap dynamics in a tropical rain forest. *Ecology*, 70(3), 555–558.
- McGraw, J. B. (1989). Effects of age and size on life histories and population growth of *Rhododendron maximum* shoots. *American Journal of Botany*, 76(1), 113–123.
- Minor, C. O. (1951). Stem-crown diameter relations in southern pine. *Journal of Forestry*, 49(7), 490–493.
- Niemann, K. O. (1995). Remote sensing of forest stand age using airborne spectrometer data. *Photogrammetric Engineering and Remote Sensing*, 61(9), 1119–1127.
- Pilon, P. G., Howarth, P. J., & Bullock, R. A. (1988). An enhanced classification approach to change detection in semi-arid environments. *Photogrammetric Engineering and Remote Sensing*, 54(12), 1709–1716.
- Pinz, A. J. (1991). A computer vision system for the recognition of trees in aerial photographs. *Multisource data integration in remote sensing, Conference NASA Conference* (pp. 111–124).
- Pollock, R. (1998). Individual tree recognition based on a synthetic tree crown image model. *International forum: Automated interpretation of high spatial resolution digital imagery for forestry, Conference Natural Resources Canada, Canadian Forest Service, Victoria, British Columbia* (pp. 25–34).
- Pouliot, D. A., King, D. J., Bell, F. W., & Pitt, D. G. (2002). Automated tree crown detection and delineation in high-resolution digital camera imagery of coniferous forest regeneration. *Remote Sensing of Environment*, 82, 322–334.
- Russ, J.C. (1995). *The image processing handbook*, 2nd Ed. Boca Baton: CRC Press. 674 pp.
- Soille, P. (2003). *Morphological image analysis: Principles and applications*. Berlin: Springer. 391 pp.
- Souto, D., Luther, T., & Chianese, B. (1996). Part and current status of HWA in eastern and Carolina hemlock stands. *Proceedings of the first hemlock woolly adelgid review, Conference U.S. Department of Agriculture, Charlottesville, Virginia, October 12, 1995* (pp. 29–60). U.S. National Institute of Health, (2003). *ImageJ 1.31*. Washington, DC.
- Usher, M. B. (1972). Developments in the Leslie matrix model. In J. N. R. Jeffers (Ed.), *Mathematical models in ecology* (pp. 29–60). Oxford: Blackwell Scientific Publications.
- Wilcoxon, F. (1945). Individual comparisons by ranking methods. *Biometrics*, 1, 80–83.
- Wulder, M., Niemann, K. O., & Goodenough, D. G. (2000). Local maximum filtering for the extraction of tree locations and basal area from high spatial resolution imagery. *Remote Sensing of Environment*, 73, 103–114.